A Preventative Approach to Mitigating CW Interference in GPS Receivers

ASGHAR TABATABAEI BALAEI is a PhD student in the School of Surveying and Spatial Information Systems, University of New South Wales, Australia. He received B.Sc and M.Sc in Electrical Engineering from Sharif University of Technology, Iran in 1998 and 2000. His current research activities are focused on the detection of interference and characterization of their effects on the Global Navigation Satellite System (GNSS).

BEATRICE MOTELLA is a Ph. D. student in Electronic and Communication Engineering. She is a member of the NavSAS (Navigation Signal Analysis and Simulation) group in the Electronics Department of Politecnico di Torino (Italy). She received the Master's Degree in Communications Engineering at the same University. Her research activity is focused on the Radio Frequency Interference (RFI) for radio-navigation systems.

ANDREW DEMPSTER, (M'95–SM'04) is Director of Research in the School of Surveying and Spatial Information Systems at the University of New South Wales. He was project manager and system engineer on the first GPS receiver to be designed in Australia and has been teaching satellite navigation for over a decade. His current research interests are in signal processing for satellite navigation, new receiver techniques and new location technologies.

Abstract - In the Global Positioning System (GPS), Code Division Multiple Access (CDMA) signals are used. Because of the known spectral characteristics of the CDMA signal, Continuous Wave (CW) interference has a predictable effect on the different Pseudo Random Noise (PRN) spreading codes (unique to each satellite) depending on the Doppler frequency of the signal. The Doppler frequency for each signal is also predictable once the receiver position is known. As different satellite signals have different Doppler frequencies, the effect on the signal quality is also different. In this paper first the effect is analytically studied. Then the concept of an "exclusion zone" is defined and analyzed for each satellite.

This exclusion zone is shown to be predictable for each satellite as a function of time. Using this prediction, the CW interference effect on the positioning quality of the receiver can be mitigated by ignoring the affected satellites within exclusion zones when performing position evaluation. The threshold, beyond which a satellite should be excluded, is then derived by studying the mutual effect of the geometry and the signal quality of that satellite on the positioning quality. Receiver Autonomous Integrity Monitoring (RAIM) uses redundancy in measurements to perform an internal consistency check to see if all of the measurements are satisfactory. In this paper this technique is also used to mitigate the effect of CW interference on the positioning accuracy. Finally it is shown that the prediction of the exclusion zone for each satellite outperforms the RAIM algorithm in mitigation the effect of the interference when 5 satellites are visible.

1. Introduction

Radio Frequency Interference (RFI) is amongst the most disruptive events in the operation of a GPS receiver. It affects the operation of the Automatic Gain Control (AGC) and Low Noise Amplifier (LNA) in the RF front-end (Kaplan (1996) Bastide (2003)) and depending on how much of it passes through these primary modules, it can also affect the carrier and code tracking loops (Betz (2001) and Tabatabaei (2005)) which results in deterioration of all the GPS observables or in complete loss of lock in severe cases. CW interference has been shown to have severe effects on the GPS C/A code signal (Spilker (1996)). This is because the frequency spectrum of the C/A code signal has a series of vulnerable lines (Kaplan (1996)). Interference can be detected in the receiver either before or after the correlation. Pre-correlation techniques use the antenna (Brown (1999)), and Analogue to Digital Converter (ADC) (Amoroso (1983)) to detect and characterize the RFI. In the post-correlation stage, the observables of the receiver that are affected by RFI have usually been used to detect and characterize the interference.

There are many different techniques for mitigation and suppression of interference. Antenna array processing, adaptive filtering (Abimoussa (2000)), time-frequency analysis and synthesis (Lijun (2005)) are among them. In Ndili (1998), interference is detected based on a combination of the following test

statistics: correlator output power, variance of correlator output power, carrier phase vacillation, and AGC control loop gain.

Receiver Autonomous Integrity Monitoring (RAIM) is also considered as another mitigation approach (Dempster (2006)). Specifically for the CW RFI which can affect one satellite at a time, this technique proves to be effective. However, our ability to predict the impact of CW RFI on the signal quality of the GPS receiver can achieve better results than simply applying RAIM algorithms. Specifically in the static applications such as Continuously Operating Reference Stations (CORS) network base stations where the environmental characteristics such as multipath and interference model do not change, this proactive approach to monitoring the satellite signal quality and availability is shown to have advantages.

In this paper in section 0 the effect of CW on the carrier to noise ratio (C/No) is analytically studied. The concept of the satellite exclusion zone is defined and characterized based on interference parameters. This work up to this stage has been already published by the authors in a non-refereed form. In section 3, the elements of satellite positioning quality is studied to obtain an appropriate threshold to determine the exclusion zone. The proactive mitigation algorithm is also presented in this section. Section **Error! Reference source not found.** is dedicated to the experiments to mitigate interference from real GPS signals collected by a software GPS receiver using both a RAIM algorithm and the proposed preventative technique and discussion about the results. Finally the paper concludes in 5.

2. The Effect of CW RFI on the GPS Signal Quality

In Tabatabaei (2006), we derived an expression for the post-correlation carrier to noise density (C/No). Figure 1 shows a block diagram of the correlation process in the GPS receiver.

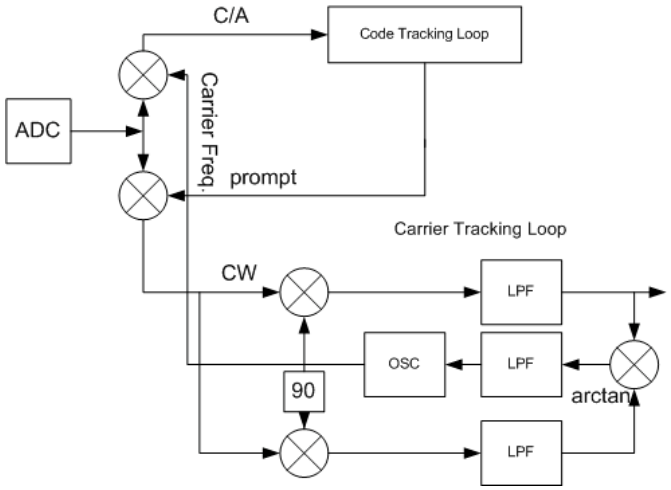

Figure 1 Correlator (Code and Carrier Tracking Loops)

Eq. 1 shows the mathematical expression for the C/No in the output of the correlator (Tabatabaei (2006)).

$$\mathrm{C/No} = \frac{(\sqrt{2P_s}T_d R_0(\tau).\mathrm{sinc}(\Delta f_c T_d))^2}{L_n N_0 + (J.T_d \mathrm{C}_\mathrm{n}^*.\mathrm{sinc}(\mathrm{T_d}.\Delta f_i))^2}$$

Eq. 1

where: P_s is the GPS signal power, No is the thermal noise power, J is the interference power. L_n is the processing gain in the noise, T_d is the integration duration time, $\hat{f}_c$ is the estimate of carrier frequency.

$\Delta f_c = f_c - \hat{f}_c$ and $\Delta f_i = f_i - f_c$, $\mathrm{C_n}$ is the $\mathrm{n^{th}}$ spectral line coefficient $R_0(\tau)$ is the cross correlation of the received C/A code and the receiver estimate of the that code and τ is the signal-reference code phase difference in code chips.

In Figure 2, as an example, using Eq. 1 and assuming a specific environmental noise power, the C/No is shown for satellite 1 with Doppler frequency changing from 0 KHz to 10 KHz and CW interference with a specific power at 14 kHz away from the band centre at L1 frequency (i.e. at 1.57552 GHz).

The deep troughs in this graph correspond to the coincidence of CW RFI with the code spectral lines. It is clear that this happens at 1 kHz spacing in the Doppler frequency. As expected from Eq. 1, there are different values for different lines. This difference comes from the difference between the coefficients of different lines in the code spectrum. This particular line spectrum would also be different for different satellite codes. The other point which is noticeable in this figure is the sinc functions occurring around each trough. The width of each sinc function

is related to the integration period, as can be seen in the Eq. 1. The longer the integration period is the narrower will be the sinc functions and the more immune the receiver will be to CW interference.

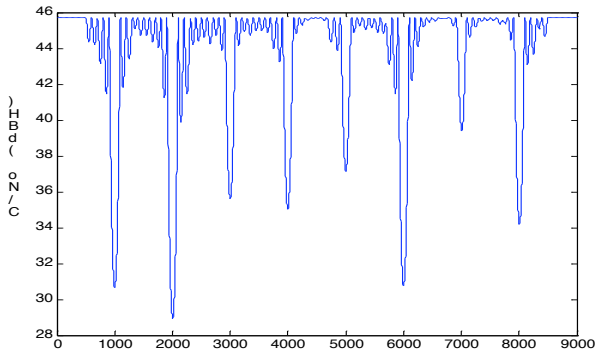

Figure 2 C/N0 calculated using the mathematical expression for satellite 1 with Doppler frequency changing from 0 kHz to 10 kHz and CW interference at 14 kHz away from L1 frequency

Figure 3 shows the variation of the Doppler frequency for different satellites for 24 hours for a specific almanac file in the presence of narrowband CW interference. Gaps in the plots indicate where an interferer in L1 frequency (or any integer multiply of 1 KHz away from that) may cause these signals to be "lost". Depending on satellite number, signal power, strength of the interference and the background noise power, the width of this gap changes. Instead of losing lock, we can set a threshold for the C/No which is a good indication of the signal quality. For any value of C/No less than this threshold, that specific signal will be taken out of the operating channels. We call the zones that are achieved through this algorithm "exclusion zones". This is the frequency region in which the interference "knocks out" that satellite and the pseudorange for that satellite should be "excised" from the solution.

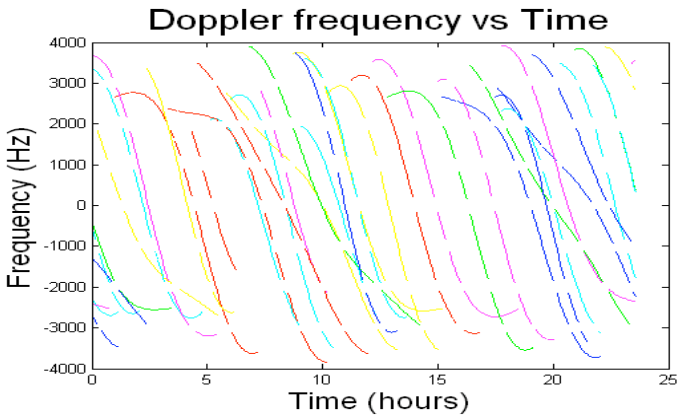

Figure 3 Variation of Doppler frequencies for the visible satellites over 24 hours. Exclusion zones are indicated at multiples of 1 kHz.

There are number of different techniques in detecting the RFI and calculating its frequency and power. Statistical inference and Fourier transform is a common technique which is used for this purpose in (Tabatabaei (2006)). Once the exact frequency of the RFI is calculated, the second step is to find the exclusion zone for each of the lines. In Figure 4 this quantity is shown in terms of the corresponding trough depth in the C/No calculated theoretically (Eq. 1).
In this case, a conservative value of 40 dBHz is chosen for the C/No threshold. Obviously the higher the line, the greater the effect of the interference, and the deeper will be the trough in the C/No. The figure shows that the deeper is the trough, the wider will be the exclusion zone of that satellite around that specific line. This graph provides an idea to calculate the exclusion zone of any satellite signal at any Doppler frequency.

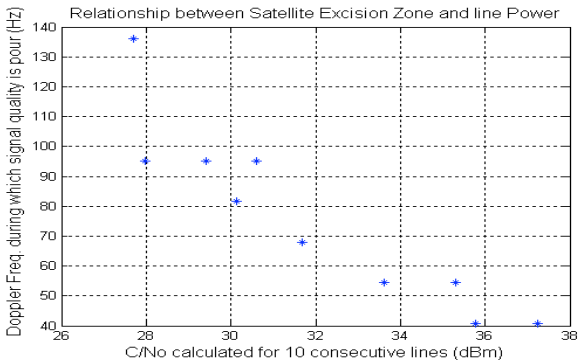

Figure 4 Relation between trough depths in C/No calculated theoretically and the corresponding satellite exclusion zone

In Figure 4, it can be seen that there is a linear relationship between the exclusion zones of different C/A code spectral lines and the C/No trough depth which is calculated theoretically as the result of those lines. In the following experiment the NordNav software receiver is used to capture the IF data to be analyzed and post processed and a signal generator (HP8648B) is used to generate the CW interference which is combined with the GPS signal generated by a SPIRENT GSS6560. The aim of this experiment is to characterize the effect of interference power on the level of C/No (Tabatabaei (2006)). The exclusion zone is characterized for just the two lines circled (9 and 10 kHz away from the band centre) in Figure 5. In this figure both the theoretical and the actual calculated C/No (using the I and Q samples from the NordNav software receiver) are shown to have the same pattern and overlapping each other.

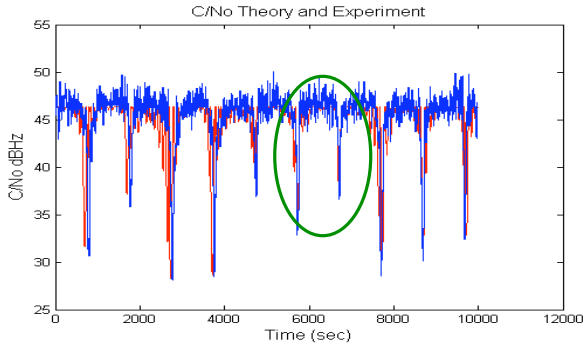

Figure 5 C/No calculated using the I and Q samples (PRN 1, interference at 4 KHz away from L1)

Instead of 10 kHz, the interference is moved only 2 kHz in 4 minutes (which guarantees one 1 kHz line in 2 minutes). In this experiment, the wideband noise power and the signal power are kept constant. The experiment is performed for four different RFI powers (Table 1).

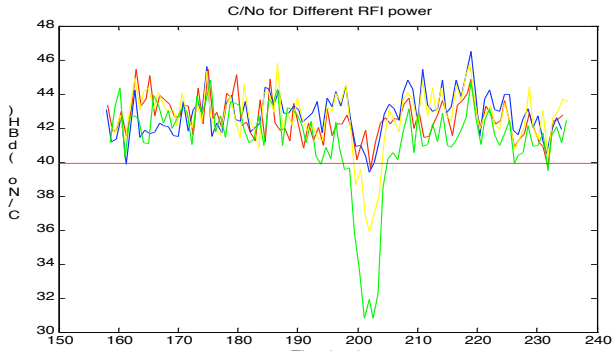

Figure 6 C/No for four different values of RFI power (green, yellow, blue and red for -82, -85, -88, -91 dBm correspondingly)

RFI Power/ exclusion zone	- 82dBm	- 85dBm	- 88dBm	- 91dBm
Line 1	94 Hz	87 Hz	22 Hz	0 Hz
Line 2	101 Hz	95 Hz	14 Hz	7 Hz

Table 1 Exclusion zones for four different RFI powers for two consecutive C/A code spectral lines

In Figure 6, the effect of these four power levels of RFI is shown on the C/No. It is obvious that where the RFI lines up with the C/A code spectral line, the higher power has the more serious effect. The other thing that can be seen from Figure 6 is that where the RFI does not line up with the C/A code line, the power of RFI does not have any effect on the C/No. In other word CW RFI affects only when it lines up with the C/A code line. In Table 1, it can be seen that the exclusion zone

for the two lines is increased with the power of RFI. This is expected, as the depth of the trough is greater for greater RFI power, and the width is also greater.

3. Positioning Quality Elements

Satellite geometry and satellite signal quality, mathematical approach

The accuracy of positioning, using the measured pseudoranges from the receiver to each of the satellites, depends on several different factors. The position evaluation in the GPS receiver estimates four quantities (x, y, z and time) using four or more pseudoranges. In other word we have the following nonlinear estimation problem (Parkinson (1996)).

$$\rho_i = |r_i - r_u| + c.b_u + \varepsilon_{\rho_i}$$

Eq. 2

where r_i is the satellite position at transmit time; r_u is the receiver position at receive time; b_u is the bias in the receiver clock, c is the speed of light and ε_{ρ_i} is the composite of errors that can be estimated from a budget (Parkinson (1996)). The states to be estimated are r_u and b_u. The linearized version of the above equation about a nominal point ($\hat{r}_u$, $\hat{b}_u$) is as follows:

$$\Delta\rho_i = G.\begin{bmatrix} \Delta r_u \\ c.\Delta b_u \end{bmatrix} + \Delta\varepsilon_{\rho_i}$$

Eq. 3

where

$\hat{1}_i = \dfrac{r_i - \hat{r}_u}{|r_i - \hat{r}_u|}$, $\Delta r_u = \hat{r}_u - r_u$, $\Delta b_u = \hat{b}_u - b_u$, $\Delta\varepsilon_{\rho_i} = \hat{\varepsilon}_{\rho_i} - \varepsilon_{\rho_i}$ and $G = \begin{bmatrix} -\hat{1}_i^T & 1 \end{bmatrix}$.

or briefly: $\Delta\rho = G\Delta x + \Delta\varepsilon_\rho$.

$\Delta\varepsilon_\rho$ is assumed to be zero mean, so that the least squares solution to the set of normal equations is given by

$$\Delta\hat{x} = (G^T G)^{-1} G^T \Delta\rho$$

Eq. 4

It is easy to see in this equation that the position accuracy is decided by two factors, the measurement quality and the user-to-satellite geometry. These factors separately are extensively discussed in (Parkinson (1996)). In this section we will make a quantitative comparison of the effect of each one of these two factors on the positioning accuracy. The aim is to establish if $\Delta\varepsilon_{p_i}$ is large because of the poor signal quality (low C/No), under which circumstances we can achieve better position accuracy by eliminating that satellite, noting the fact that eliminating the satellite will affect the geometry.

To achieve this goal, we simplify the scenario. The assumption is that there are 5 satellites available to the receiver and of these only one has affected signal quality. This situation is likely to occur when there is moderate blockage of sky and a single CW interferer is present. The position error covariance is studied in this investigation: $\mathrm{cov}(\Delta x) = E(\Delta x \Delta x^T)$ where *E(.)* operates as an expected value operator. From Eq. 4 we have:

$$\mathrm{cov}(\Delta x) = E((G^T G)^{-1} G^T \Delta\rho \Delta\rho^T G (G^T G)^{-1})$$

Eq. 5

At this stage two different cases are considered: 4 satellites all having the same pseudorange error (ε) and 5 satellites one of which signal is degraded and has larger pseudorange error (η). Without loss of generality we can assume here that the pseudorange error in the first case for each satellite is 1 m and that of the second case to be $\xi = \eta / \varepsilon$. Then for the two cases we will have:

$$\mathrm{cov}_4(\Delta x) = (G_4^T G_4)^{-1} (G_4^T W_4(\xi) G_4)(G_4^T G_4)$$

Eq. 6

where $W_4(\xi) = I_4$

and

$$\mathrm{cov}_5(\Delta x) = (G_5^T G_5)^{-1} (G_5^T W_5(\xi) G_5)(G_5^T G_5)$$

Eq. 7

where $W_5(\xi) = \begin{bmatrix} I_4 & 0 \\ 0 & \xi^2 \end{bmatrix}$.

G_4 and G_5 represent the G matrix respectively for the cases of 4 and 5 satellites.

The difference between the above two quantities comes from the difference between G_4 and G_5 on the one hand and W_4 and W_5 on the other. In the scenario explained in the following section, the effects on the position error covariance of W and G are studied.

The data used for this scenario is a set of real data collected with a GPS software receiver NordNav-R30 at the University of the New South Wales on the 6th November 2006. 6 satellites (1, 11, 20, 23, 25 and 31) are acquired by the receiver.

To compare the covariance matrices (Eq. 6 and Eq. 7), one way is to compare their determinants. Two satellite sets of (1, 23, 25, 31) and (1, 11, 23, 25, 31) are chosen. These two sets are chosen because during the initial epochs of the data, satellite 11 plays a fundamental role in delivering good geometry of the constellation. In this experiment, as explained earlier, only the pseudorange error of the satellite 11 is changed. By using Eq. 6 and Eq. 7, the amount of pseudorange error of satellite 11, which makes the position error for the two configuration equal, is found to be $\xi_0 = 22\,m$. Figure 7 shows the position error for the two cases. It is clearly seen that the position error for the two configurations (4 satellites and 5 satellites) become equal to each other at $\xi_0 = 23.1\,m$ which is very close to what is achieved theoretically.

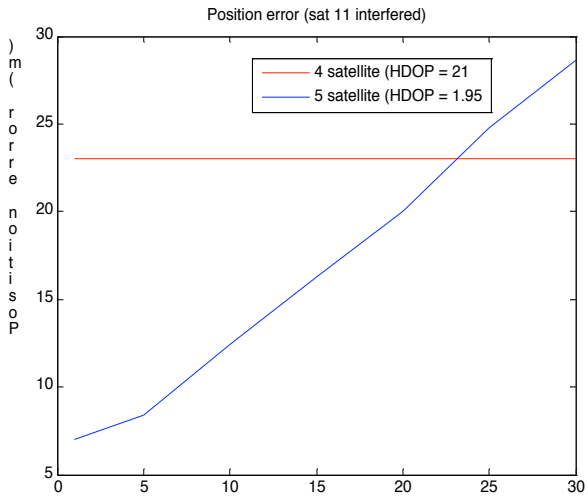

Figure 7 Position error vs. pseudorange error for the 4 and 5 satellite configuration at a particular time

In another scenario, another two satellite sets are chosen which have very similar and good geometries. These two sets are (1, 11, 20 and 23) and (1, 11, 20, 23 and 25). The satellite of which the pseudorange error has been increased is satellite 25.

Again using Eq. 6 and Eq. 7, the pseudorange error at which the two position error become equal is calculated. This error is found to be $\xi_0 = 1.45\ m$. Figure 8 shows that this value in experiment is 1.65 *m.* This means that there will be times when eliminating the satellite because of its poor CN0 will have advantages and others when the degradation has to be significant before elimination helps.

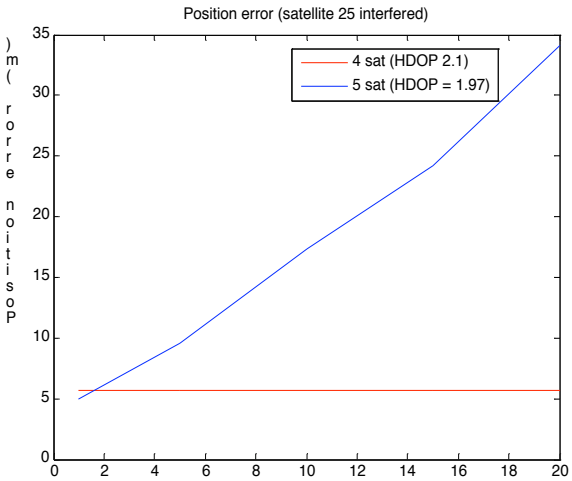

Figure 8 Position error vs pseudorange error for the 4 and 5 satellite configuration

Mitigation algorithm description

Here the algorithm for the proposed technique to mitigate the effect of CW interference is described.

1) As was explained in section 0, using the information regarding the frequency and power of the interference and the constellation information, the carrier to noise ratio of each channel is predicted using Eq. 1.
2) Using Eq. 6 and Eq. 7, the minimum pseudorange error for each of the satellites in view at which the positioning error is higher when including that particular satellite rather than omitting it is found. This value is called ξ_0. Here it is assumed that the relationship between the pseudorange error and the carrier to noise ratio for the GPS receiver in which this algorithm is used, is known (Ndili (1998)).
3) If the predicted carrier to noise ratio of a satellite is less than the value which corresponds to ξ_0 m pseudorange error, then that satellite will be excluded from the positioning evaluation.

This process is schematically shown in Figure 9.

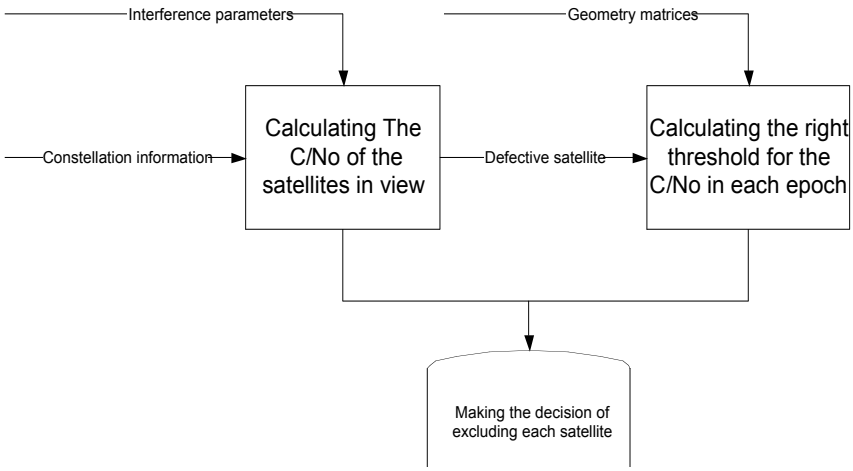

Figure 9 Algorithm description flow chart

It was shown in section 0 that degradation in satellite signal quality (C/No) due to interference can prevent one or more satellites at a time being available. In Fante (2000) the probability of availability of N satellites in the presence of interference in terms of C/No was investigated. Due to the nature of this impact of CW RFI on the GPS satellite signals, one can reasonably think of using a RAIM algorithm to mitigate this effect. In Kim (2006) the position domain errors are assessed with the use of traditional least-squares estimation in the presence of interference, mitigated by a RAIM scheme.

In this section the dependency of our proposed mitigation algorithm on the satellite geometry was studied. In Brown (1990) the dependency of RAIM on geometry is discussed. In the next section using some experiments these two mitigation techniques are presented through some experiments and the results are analyzed and discussed.

4. Experiments Discussion and Results

The impact of the HDOP

The goal of this section is to demonstrate the theoretical analysis discussed in sections 2 and 3 with some experiments. The data used for this purpose are the same of those have been used for the simulation results. The question to be addressed is in which cases the ‘exclusion zones’ algorithm can be applied. In other words: what is the trade-off between the loss of positioning accuracy due to degraded geometry and a loss of position accuracy due to the use of the satellite

affected by CW interference? This is then used to decide if the affected satellite should be eliminated from position estimation. By analyzing the following two examples this question is approached.

In the first example we analyze the possibility of applying the 'exclusion zone' algorithm in the case where the HDOP is comparable before and after excluding one satellite. The constellation considered is composed of satellites 1, 11, 20, 23 and 25. The CW interference affects the signal of satellite 1. It can be seen from Table 2 that the value of the HDOP does not change significantly when satellite 1 is removed. In fact the HDOP stays almost constant for the 38 minutes of data.

HDOP (m) – 5 sat	HDOP (m) - 4 sat
1.97	2.07

Table 2 HDOP for the 5 and 4 satellite configuration

The position error is described versus time (Figure 10 (a)) and on the scatter diagram (Figure 10 (b)). Blue lines refer to the 5 satellite configuration, while red lines refer to the position error evaluated omitting satellite 1.

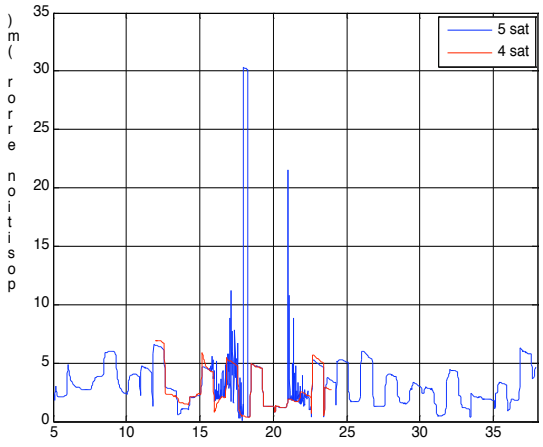

(a)

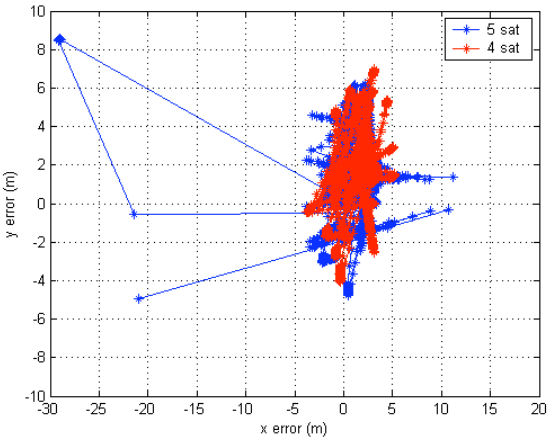

(b)

Figure 10 Position error vs. time (a) and scatter diagram (b). The comparison is between the 5 satellites configuration (blue line) and the 4 satellite one (red line) when the interference affects the satellite 1 (kept out in the 4 sat configuration**)**

It is observed that the performance of the 4 satellite configuration is comparable with the 5 satellite ones, except where the interference matches one of the lines of the PRN 1 code (between min 16 and min 22). In this time interval in fact the 5 satellite configuration presents a very high error level (up to 30 m), while the 4 satellite configuration is immune from it. This example shows that when the HDOP does not suffer a significant loss when omitting the satellite affected by interference, the application of the 'exclusion zone' algorithm is able to mitigate the presence of the interference.

On the contrary, the second example analyses the case where the HDOP varies significantly after removing one satellite. The constellation is composed of satellites 1, 11, 20, 25 and 31. The CW interference affects the C/No of the satellite 11 (Figure 11 (a)). Moreover in the 4 satellites configuration the value of

the horizontal dilution of precision varies from 22.5 to 4 m during the 38 minutes (Figure 11 (b)).

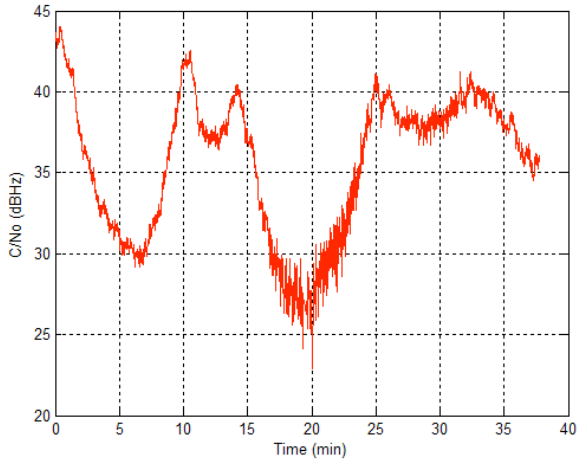

(a)

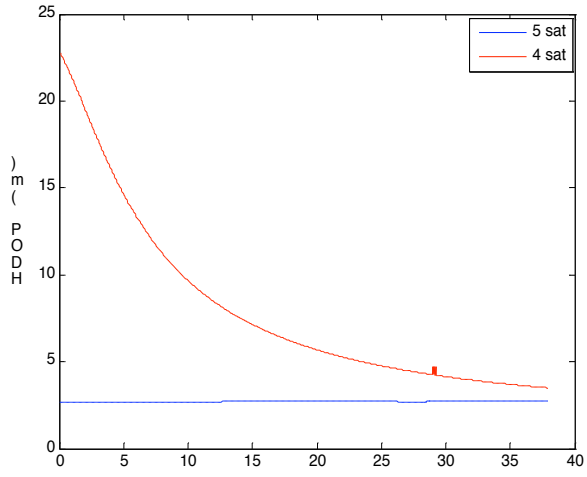

(b)

Figure 11 C/No for the PRN 11 (a) HDOP for the 5 and 4 satellites configuration (b)

During the first 18 minutes the difference between the HDOP of the two constellations is very high. This means that the HDOP of the 4 satellite configuration is extremely high and this is reflected in a very high position error. The maximum error in this case is 35 m and it exceeds 15 m several times. With this level of position accuracy there is no reason to apply the exclusion zone algorithm, because the HDOP does not allow having acceptable position estimation.

On the contrary, when the difference in HDOPs is not significant (less than 7 m – after min 18), it is easy to observe that the performance of the 4 satellite configuration, after the application of the exclusion zone algorithm, is much better than the 5 satellites configuration when the interference matches one of the line of the PRN 11 code (Figure 12 (a)). In order to see how much the interference can

affect the position accuracy Figure 12 (b) represents the difference with and without interference.

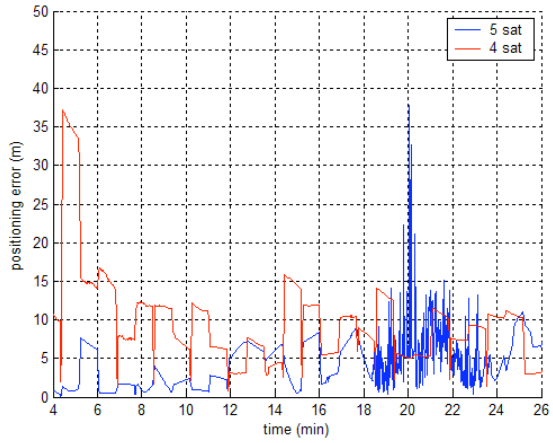

(a)

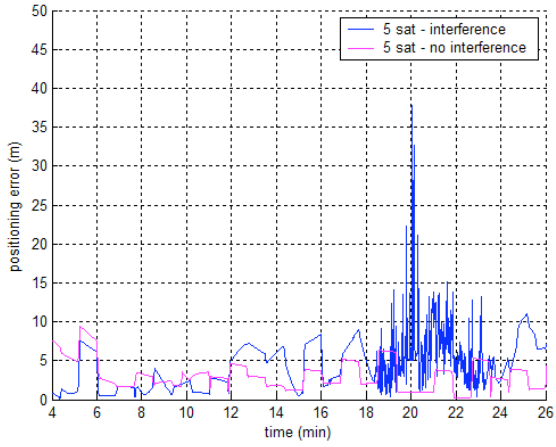

(b)

Figure 12 Comparison between the positioning error using 5 and 4 satellites in presence of interference (a) Comparison between the positioning error using the 5 satellites constellation with and without interference (b)

Exclusion Zone – RAIM Comparison

In order to show the advantages of the 'exclusion zone' algorithm and make a comparison between this technique and a RAIM technique, an example is shown. More specifically the maximum separation of solution method (Parkinson (1996)) has been chosen for the comparison.

To apply the exclusion zone algorithm, we consider the example in previous subsection, (Figure 10). In Figure 13 (b), which is the trend of the C/No of satellite 1, it is observed that the decision to keep out the satellite can not be based only on measuring the actual C/No level. This level is in fact always quite high (> 34 dBHz) even when the position quality is severely affected by the interference.

This is explained in Tabatabaei (2006) where the behavior of C/No in the presence of CW interference is characterized. It is shown that this type of interference has an "improved" effect on the C/No, when its frequency is very close to the frequency of one of the lines of the C/A code. The reason is that the carrier tracking loop tracks the interference and the stronger the interference is the higher will be the C/No. On this basis, the C/No by itself can be a misleading indicator in this specific situation.

Instead of monitoring the C/No, by predicting the C/No this problem is resolved. In this experiment the frequency of the CW RFI is chosen so that the signal of GPS satellite 1 is affected significantly during the course of the 38 minutes. The Doppler frequency of this satellite is shown in Figure 13 (a). The interference is chosen to be at frequency 12.1 kHz away from L1. As the Doppler frequency of this signal is 2 kHz, so the RFI will coincide with the 10^{th} spectral line of this code in the middle of the experiment. The RFI power is chosen to be -82 dBm because this guarantees C/No degradation – see Table 1.

In section 3, we proposed a method to calculate, at any given time, the C/No threshold ξ_0 at which a satellite should be excluded. Following that analysis, ξ_0 for this specific case is 2.1 m. In the next step the carrier to noise ratio, corresponding to this level of pseudorange error should be found. In (Ndili (1998)) the relationship between pseudorange error and the correlator output power or the C/No is characterized. This relationship varies based on the receiver. The fact that ξ_0 is very close to 1 m means that satellite 1 does not have a significant effect on the geometry and therefore should be excluded from the positioning calculation as soon as the positioning error is affected by the poor signal quality. For this specific PRN code line and RFI power level and the threshold, the exclusion zone from Eq. 1 is found to be 101 Hz (Figure 13).

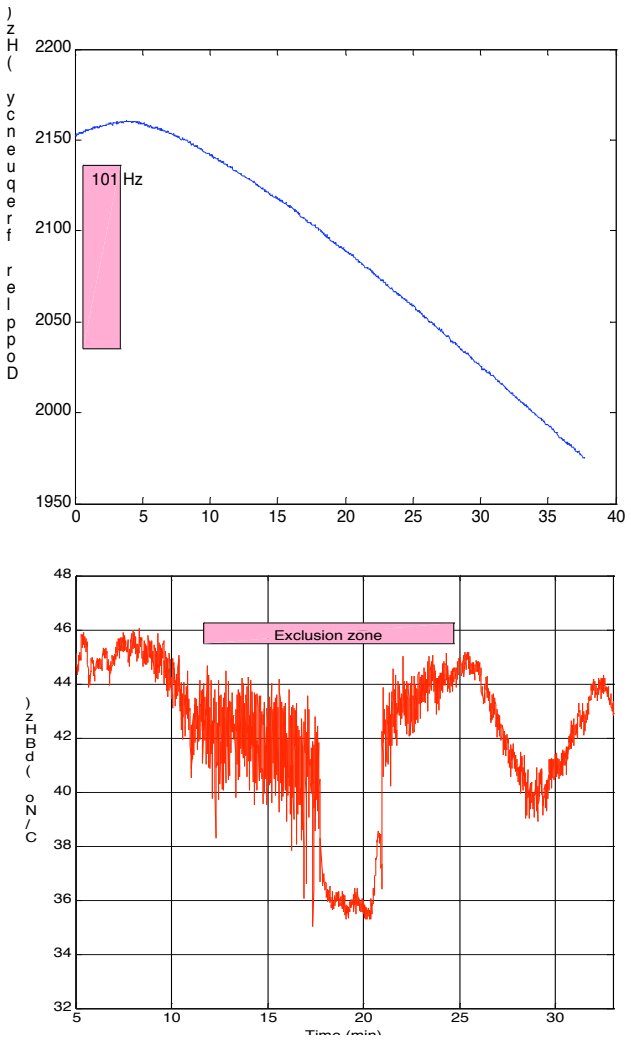

Figure 13 (a) Doppler frequency for satellite 1 (b) Exclusion zone for PRN 1

As we saw in the example (Figure 13), the advantages of the algorithm are appreciable when we have only 5 satellites in view. This can be explained by considering the fact that using Eq. 6 and Eq. 7, the pseudorange error for satellite 1 to degrade the positioning error (ξ_0) is very high. In other word the threshold for the C/No for the exclusion zone is very low. The experiment shows how the exclusion zones algorithm can deliver advantages in terms of position accuracy. We now compare its performance to the RAIM algorithm.

As Section **Error! Reference source not found.** describes, RAIM needs at least 5 satellites to detect the presence of an error in one of the pseudorange and 6 satellites to identify which is deficient.

In order to compare the exclusion zones algorithm with RAIM, the situation with 5 satellites in view is analyzed. Figure 14 shows the maximum distance between

the 5 position solutions evaluated removing one satellite at a time (constellation: PRN 1, 11, 23, 25, 31).

In this case it is difficult to detect the presence of the error using the maximum distance of solutions algorithm. The different positions are evaluated using only 4 satellites. This means that the HDOP can significantly affect the accuracy in the positioning evaluation. Therefore in this experiment, even though 5 satellites are available, because of poor geometry, even the presence of error caused by interference can not be detected.

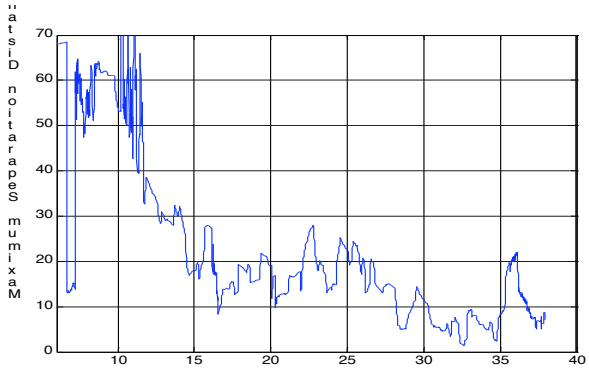

Figure 14 Maximum distance between positioning from different satellite configuration

5. Summary

In this paper a new technique to mitigate the effect of CW interference on GPS C/A code signal quality is introduced. No analogue or digital filter is used in this algorithm and this helps keep the GPS signal phase and amplitude from being distorted. Unlike other mitigation techniques which are responsive, this technique works preventatively but it does require knowledge of the interference frequency and power, which may be estimated by known techniques. This means that it predicts and prevents the error before it happens. The specific signal structure in GPS allows us to predict the effect of CW interference on each of the satellites' signal at any given time. It usually affects one signal at a time and in the technique proposed in this paper that affected signal is removed from the positioning calculations provided that its effect on the user-to-satellite geometry on the positioning quality is less than that due to the poor signal quality of that particular satellite.

Receiver autonomous integrity monitoring techniques work on a similar basis. The difference is that in the RAIM approach the affected signal is detected after

the error appears in the positioning calculations. In this paper the results of that mitigation is compared with our preventative mitigation approach.
The other advantage for the new technique is when the receiver receives 5 satellites, RAIM is unable to eliminate the bad satellites so either the position is ignored or the bad position is used whereas our proposed proactive RAIM method allows a "good" 4 satellite solution.

Reference

Abimoussa R, Landry RJ (2000) Anti-jamming solution to narrowband CDMA interference problem. Canadian Conference on Electrical and Computer Engineering.

Amoroso F (1983) Adaptive A/D Converter to Suppress CW Interference in DSPN Speard-Spectrum Communications. IEEE Transaction on Communications

Bastide F, Macabiau C, Akos DM (2003) Automatic Gain Control (AGC) as an Interference Assessment Tool. Proceeding of ION GPS/GNSS

Betz JW (2001) Effect of Partial-Band Interference on Receiver Estimation of C/N0: Theory. Proceedings of ION.

Brown A, Reynolds D, Roberts D, Serie S (1999) Jammer and Interference Location System-Design and Initial Test Results. Proceedings of the ION GPS.

Brown A, Sturza M (1990) The effect of geometry on integrity monitoring performance. Proceedings of the ION.

Dempster A (2006) How Vulnerable is GPS?. Position 20: 64-67.

Fante RL, Vaccaro JJ (2000) Ensuring GPS availability in an interference environment. Position Location and Navigation Symposium IEEE.

Kaplan E (1996) Understanding GPS: Principles and Applications. Artech House.

Kim N (2006) Interference Effects on GPS Receivers in Weak Signal Environments. University of Calgary, Department of Geomatics Engineering Masters Thesis.

Lijun W, Huichang Z, Gang X, Shuning Z (2005) AM-FM interference suppression for GPS receivers based on time-frequency analysis and synthesis. IEEE International Symposium on Microwave Antenna, Propagation and EMC Technologies for Wireless Communication.

Ndili A, Enge P (1998) GPS receiver autonomous interference detection. Position Location and Navigation Symposium, IEEE.

Parkinson BW, Spilker JJ Jr (1996) Global positioning system: Theory and Applications. Volume I. American Institute of Aeronautics and Astronautics, Inc.

Parkinson BW, Axelrad P, Enge P (1996) Global positioning system: Theory and Applications. Volume II.

Spilker J, Natali F (1996) Global Positioning System: Theory and Applications. AIAA.

Tabatabaei Balaei A, Barnes J, Dempster AG (2005), Characterization of interference effects on GPS signal carrier phase error. Proceedings of SSC.

Tabatabaei Balaei A, Barnes J, Dempster AG (2006) A Novel Approach in the Detection and Characterisation of CW Interference on the GPS Signal Using the Receiver CN0 Estimation. Proceeding of IEEE/ION PLANS, San Diego.

Tabatabaei Balaei A, Dempster AG (2006) A Statistical Inference Technique for GPS Interference Detection. Submitted to the IEEE Transaction on Aerospace and Electronic systems.

Tabatabaei Balaei, Dempster AG, Barnes J (2006) Exclusion zones for GNSS signals when reconfiguring receiver hardware in the presence of narrowband RFI. Submitted to IAIN / GNSS, Korea.